Failure Analysis of Fixed Drive Link of Flap Track Fairing (Canoe #8) of a Wide Body Aircraft

Nanang Yulian[1], Arif Sugianto[1], Geowana Yuka Purmana[2], Arif Basuki[2]

[1]Dept of Aircraft Engineering, Engineering Services
GMF Aero Asia, Soekarno-Hatta Intl Airport, Tangerang 19103
Tel: +62-21-550-8008, Fax: +62-21-550-1282
[2]Dept of Material Engineering, Faculty of Mechanical and Aerospace Engineering
Bandung Institute of Technology, Jl. Ganesha 10, Bandung 40132
Tel: +62-22-250-2265, Fax: +62-22-250-8144
n.yulian@gmf-aeroasia.co.id; arifs@gmf-aeroasia.co.id; geo_2589@yahoo.com; arifbasuki@material.itb.ac.id

Abstrak

The failure analysis has been performed on fractured fixed drive link of flap track fairing (Canoe) #8 in drive system secondary door of a wide body aircraft. The fixed drive link is made from Aluminum Alloy 7075 per CMM 27-51-31 and OES test result. To support the analysis, laboratory practices including visual fractography, Optical Emission Spectrometry (OES), stereo microscopy, Scanning Electron Microscopy (SEM), Energy Dispersive Spectrometry (EDS), tensile test, and hardness test were conducted. The evidence shows that the fracture is initiated from area of the circle radius of fixed drive link. Beachmark is clearly observed at fractured surface as indication of fatigue failure. Final fast fracture of the fixed drive link impacted on spontaneous crack in the downstream of the drive system and also resulted in deformed forward door link. The tensile strength and hardness of the component are below the standard of AA 7075-T6 alloy. Quantitative stereo metallography shows higher percentage fraction of undesired constituent particle on the area adjacent to crack origin indicating that the homogenization process of the fixed drive link was not performed well. Hence, the causal factor of this failure is combination factors among improper manufacturing process, stress raiser due to geometry factor, and improper installation of maintenance practice on the adjustment of rod and support fitting.

Keywords: **Failure Analysis, Flap Track Fairing (Canoe), Forward Door Link, Fatigue Failure, AA 7075-T6**

1. Introduction

Daily inspection on 6 March 2011 reported that canoe was broken due to struck down by failed various components from drive system of flap track fairing. The components of drive system of flap track fairing (canoe) number 8 are Drive Rod (P/N 65B15950-1), Fixed Drive Link (P/N 65B15694-10), Forward Door Link (P/N 69B14186-1), Adjustable Rod (P/N 65B16688-1), Support Fitting (65B17001-1), Door Fitting (P/N 65B15957-2), and Secondary Door (P/N B6515690-51). The failed components were Fixed Drive Link, Forward Door Link, Adjustable Rod, and Secondary Door. Due to the multiple components failure, the analysis must be started from observed part which failed at the first time or as origin of failure.

Fig.1 Location of installed Fixed Drive Link of Flap Track Fairing (canoe) #8 [1]

Fig.2 Failed components of drive system of secondary door on canoe #8

Fixed Drive Link is hinged to flap track. When the Flap Carriage pushes the midflap to extend, the midflap also pushes the Drive Rod to drive the Fixed Drive Link. Furthermore, Fixed Drive Link moves will drive Support Fitting, Adjustable Rod and Forward Door Link to push the Door Fitting and Upper Door Link. In the end, the upper door link will move down (opened) when the flap is extended and moves up (closed) when the flap is retracted.

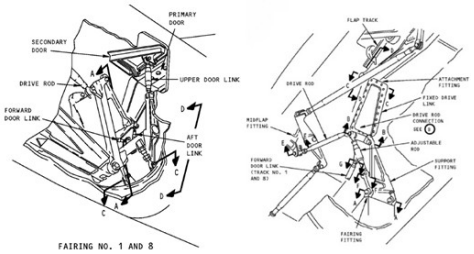

Fig.3 Drive System Configuration of Secondary Door on Canoe #1 and #8 [1]

The drive system of flap track fairing is only applied on fairing number 1 and 8. The rest of fairing (number 2 through 7) only has Drive Rod, Fixed Drive Link, Support Fitting, and Adjustable Rod inside them.

Many factors can be a cause of failure in this drive system, such as defective materials, improper installation, and corrosion environment [5]. The investigation should be started from observation on all fracture surfaces in all failed components to obtain possible crack initiation. Hence, the combination of evidence and up and down stream linkage mechanism can lead to the origin of failure.

2. Experimental Methodology & Analysis

2.1. Linkage Mechanism and Visual Fractography

There are total four failed parts in the secondary door drive system. The connection between each parts and location of fractures are illustrated in Fig.4.

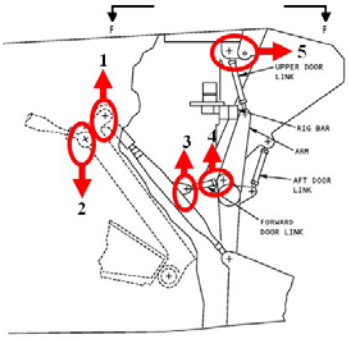

Fig.4 Connection between failed parts and position of fractures [2] [3]

The fracture surface for each failed component can be seen from Fig.5 to Fig.8. The photo was taken by DSLR camera using macro-lens. The purpose of this step is to find the features such as fatigue beachmark, chevron mark, overload, or deformation due to collision from the mating surface [5].

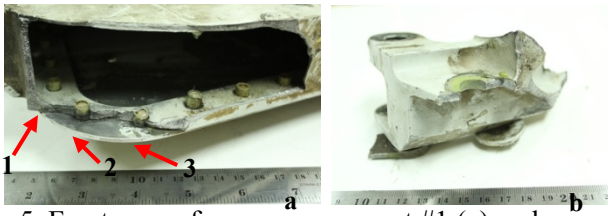

Fig.5 Fracture surface on component #1 (a) and component #2 (b)

Fig.6 Fracture surface of component #3 from Fig.4. The Adjustable rod components were broken and split into two parts

Fracture in Component #1 can be seen in Fig.5a. It shows multiple crack initiation. A dirty surface condition indicates that the crack has been there long time since dirt or grease can infiltrate into the narrow gap. A beachmark feature also can be found in the corner area (shown by the red arrow 1 in Fig.5a. The two blind fasteners also can be suspected as crack initiation based on previous cases in the same components [12].

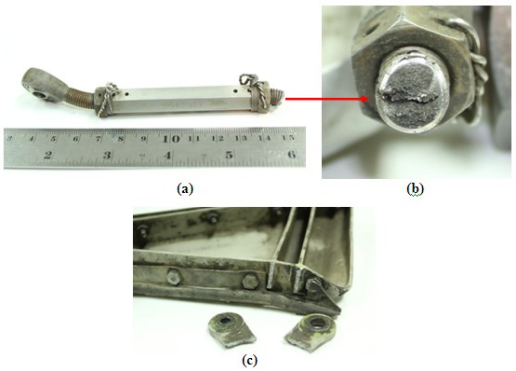

Fig.7 Failed component #4 in Fig.4. The deformed component (a), its fracture surface (b), and component #5 from Fig.4

Fracture surface shown in Fig.5b, Fig.6 and Fig.7c show rapid fracture. The macro-photography shows no feature of fatigue failure on fracture surface. The deformed Forward Door Link (Fig.7a) shows that the component sustained overload force. The overload encountered by Forward Door Link can arise from damage of other components previously. There are also no special features of fatigue failure, obtained from its fracture surface [7]. From this step we can determine that failed component #2, #3, #4, and #5 of Fig.4 are not the origin of failure in the drive system. Therefore, the next investigation was focused on failed Fixed Drive Link. Since there were three possibilities of crack initiation area, the further macro-photograph should be taken in those areas. The results can be seen in the Fig.8.

Fig.8 Crack initiation suspect areas from (Fig.5) arrow 1 (a), arrow 2 (b), and arrow 3 (c)

2.2. Chemical Composition Analysis

Based on B oeing's Components Maintenance Manual (CMM) 27-51-31 [2], the Fixed Drive Link is made from aluminum alloy. The chemical composition examination was determined by Optical Emission Spectrometry (OES). This examination is important for comparing the actual against the standard (chemical

properties, production process, and corrosion resistance of the components).

Table 1. Chemical Composition of Failed components compared to AA-7075 standard [4]

Element	Composition (%)	7075 (% w)[4]
Si	0,131	0,4 max
Fe	0,191	0,5 max
Cu	1,624	1,2 – 2,0
Mn	0,008	0,3
Mg	1,894	2,1 – 2,9
Zn	5,697	5,1 – 6,1
Ti	0,014	0,2 max
Cr	0,166	0,18 – 0,28
Ni	0,006	0,05
Pb	0,001	0,05
Sn	0,001	0,05

Aluminum alloy 7075 was chosen due to its typical use as aircraft structural where very high strength and good corrosion resistance is required.

2.3. SEM Fractography

Fig.9, Fig.10, and Fig.11 depict a SEM (Scanning Electron Microscope) photography taken from the fracture face of failed Fixed Drive Link. The fractographs were taken from JSM-6510LA SEM machine, equipped with an EDX microanalysis system from JEOL Inc.

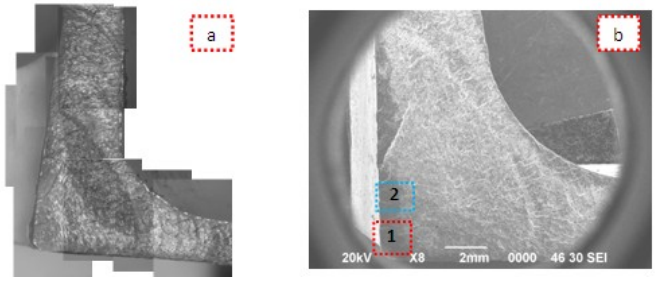

Fig.9 Fractograph of part (Fig.8a) using stereo microscope (a), and low magnification SEM (b).

The observation on fracture surface using higher magnification SEM was performed to determine the crack initiation and crack propagation area. In the crack initiation area shown in Fig.10, there is no evidence of mechanical damage, local deformation, or corrosion. Fig.11a shows difference feature of fracture surface between crack initiation and propagation.

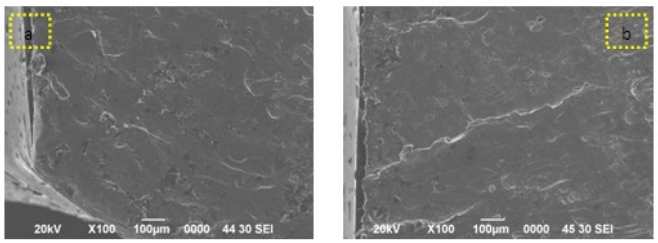

Fig.10 SEM images of area 1 (a), area 2 (b) from Fig.9b

On the crack propagation area, as shown in Fig.11b, the morphology of fracture surface shows many elongated dimples with open-end rim. The striation can also be found on crack propagation area, as shown in Fig.12.

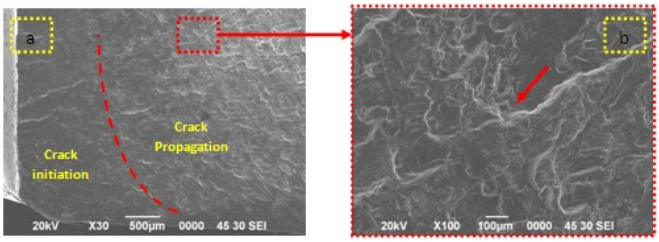

Fig.11 Fracture surface difference between crack initiation area and crack propagation area (a), showing dimple morphology (b)

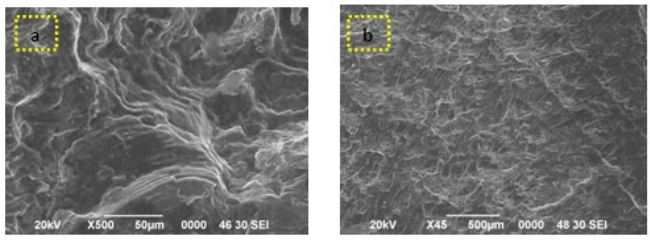

Fig.12 Striation on crack propagation, magnified from arrow in Fig.11b. (a) Fracture surface near the final failure area showing combination of dimple and cleavage (b)

The fracture surface of other possibility areas of crack initiation shown in Fig.13 does not reveal the features as crack initiation areas. The fast/ final fracture areas are combination of dimple and cleavage which show a random direction.

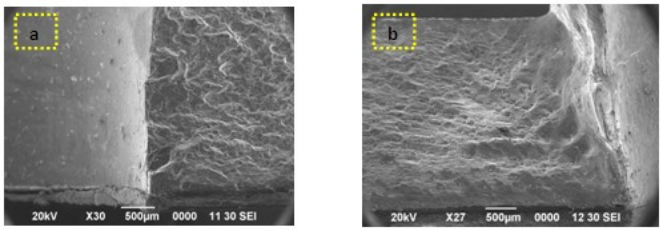

Fig.13 SEM image of fracture area of part in Fig.8b (a), Fig.8c (b)

2.4 Metallography Analysis

Microstructure analysis was performed intensively on crack initiation area in Fig.9. The surface adjacent to fracture surface was grinded, polished, and etched to reveal its microstructure [6]. The analysis was also performed on a rea sliced in every 5 mm from crack initiation area to get the microstructure comparison. Microstructures of the component were observed under optical microscope and SEM with back scattered electron image. The analysis of phase and constituent were also performed with Energy Dispersive Spectroscopy.

The distribution of insoluble phase or constituents in Aluminum matrix was also examined using Rax Vision image analysis software. The result is shown in Fig.15 and Fig.16. The result of insoluble phase percentage in

aluminum matrix under stereo micrograph quantitative metallography (Fig.15), there are 3.06% (area #1); 3.17% (area #2) and the result under SEM quantitative fractography (Fig.16), there are; 0.76 % (area #a), 0.58 % (area #b), and 0.39 % (area #c), respectively.

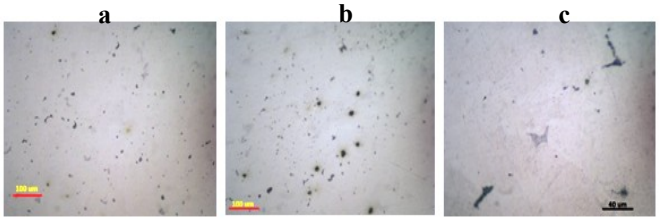

Fig.14 Un-etched microstructure from area far from initial fracture (a & b), area adjacent to initial fracture (c), under stereomicroscoupe

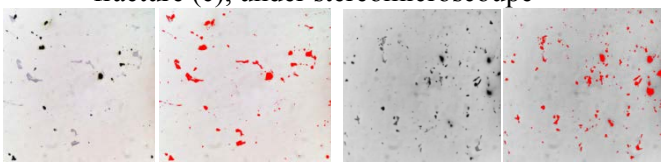

Fig.15 Un-etched microstructure on area adjacent to initial fracture (a&b) showing fraction of insoluble phase under Rax vision analysis

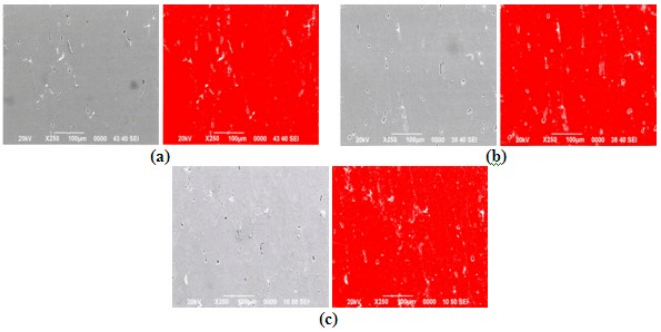

Fig.16 Un-etched SEM microstructure on area far from initial fracture under Rax vision analysis

Fig.17 shows microstructure examination under EDS illustrating the composition of the element in insoluble phases and constituents in aluminum matrix. Most of the elements are in grain boundary with high level of element Cu or Fe.

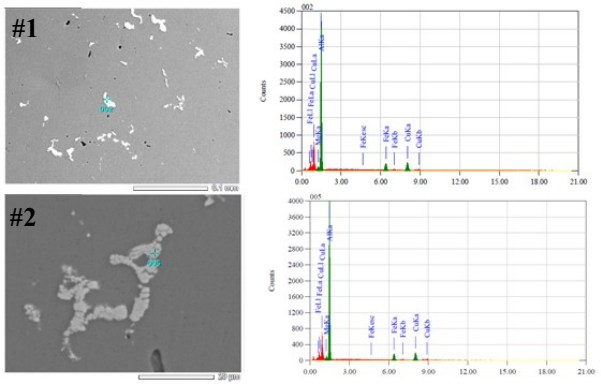

Fig.17 EDS result for insoluble phases in the area far from the crack initiation showing similar composition of constituents

Table 2. Result of EDS analysis of various types intermetallic phases shown in Fig.17 (mole fraction, %)

Position	Al	Cu	Fe	Mg
#1	65.60	23.40	9.83	1.17
#2	66.34	22.57	9.72	1.36

The EDS result for area adjacent to crack initiation shows the constituent with high percentage of Cu. Elements composition of this constituent is difference with the composition of constituent in the area far from crack initiation.

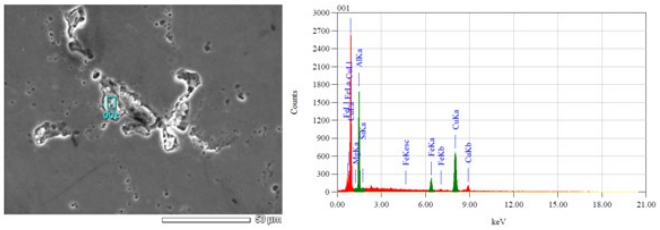

Fig.18 EDS result for insoluble phases in the area far from the crack initiation shows similar composition of constituents

Table 3. Result of EDS analysis of various types intermetallic phases shown in Fig.18 (mole fraction, %)

Position	Al	Cu	Fe	Mg	Si
#1	19.63	44.79	6.20	0.36	0.14

2.5. Mechanical Testing

Tension test and hardness test were performed to determine the mechanical properties of failed Fixed Drive Link. This step can confirm the mechanical properties of components material compared to design drawing. The specimen for tension test was made per ASTM E8 for plate. Hardness test was performed using Rockwell B method per ASTM E18.

Table 4. Tensile test result

Specimen	Tensile Strength (MPa)	Elongation (%)
A	474	12.0
B	471	12.0

Hardness test were performed to compare the hardness in the area adjacent to crack initiation and the area far from the crack initiation. The results are shown in Table 5.

Table 5. Hardness test result

Test	Fracture Area	Specimen 1	Specimen 2
1	77,9 HRB	80,1 HRB	79,5 HRB
2	81,1 HRB	79,2 HRB	80,3 HRB
3	80,9 HRB	80,0 HRB	80,5 HRB
4	80,5 HRB	80,9 HRB	80,0 HRB
5	-	82,4 HRB	81,3 HRB
Average :	**80,1 HRB**	**80,52 HRB**	**80,32 HRB**

The tensile strength of failed component is below the standard, 530 MPa, for 7075-T6. The hardness of component is also below the standard. The hardness for

7075-T6 is 150 HB (Brinell), using conversion table in ASTM E140, the Rockwell B Hardness for this material should be 89 HRB.

3. Discussion

The Fixed Drive Link component was confirmed made by 7075 Aluminum alloy based on the chemical analysis data on Table 1. Aluminum alloy series 7xxx have Zinc as their main alloying elements; alloys in this series are heat treatable [11]. The main processes of manufacturing the component from Aluminum ingot are described below.

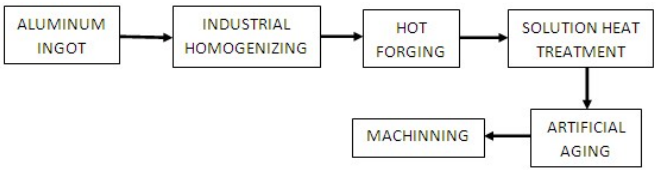

Fig.19 Production process of component from ingot of Aluminum alloy [8,9, 10,11]

As-cast aluminum ingot has segregated composition and structure with dendritic α phase and lamellar eutectic formed between dendrite [11]. Although the composition of alloying elements is in hypoeutectic, the eutectic structure can be formed. The forming of eutectic structure is possible due to non-equilibrium solidifications that were explained by Porter and Easterling [14]. The microstructure of as-cast Al-Mg-Zn-Cu alloy is shown in Fig.20.

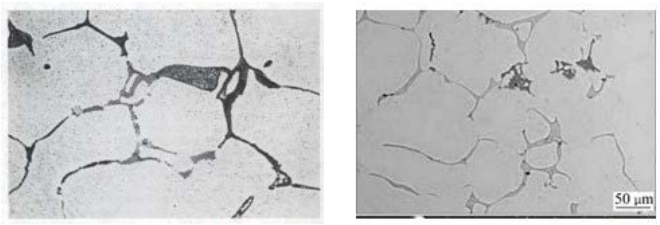

Fig.20 Microstructure of as-cast Al-Mg-Zn Cu alloy ingots. A darker area shows a grain boundary with higher content of alloying elements [11, 14].

Homogenizing or Ingot Pre-Heating is a process to improve hot workability alloy by reducing the composition segregation in as-cast ingot. The industrial homogenization temperature for 7075 is 470° C and hold for 48 hours [13]. The microstructure of homogenized Aluminum alloy can be seen in Fig.21a. Due to reduction of segregation, the alloying elements such as Mg, Zn, Cu, and Fe that formed eutectic structure in as-cast ingot can dissolve into Aluminum matrix when homogenization occurs. The enhancement of alloying content especially Mg, Zn, and Cu can increase the strength of materials due to the enhancement of strengthening precipitates formed during solution heat treatment and artificial aging. The microstructure of failed Fixed Drive Link on Fig.21b shows that the material contains many second-phase constituents. The amount of second-phase particles in the failed component is higher than the microstructure of industrial homogenized Aluminum as shown in Fig.21a.

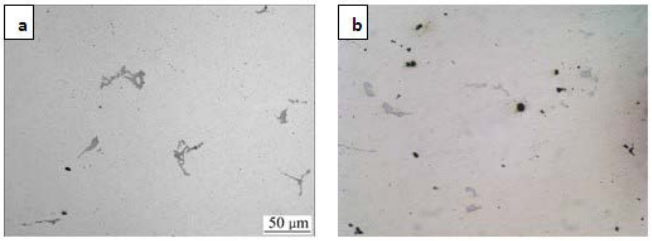

Fig.21 Un-etched microstructure of (a) Industrial homogenized Al-Zn-Mg-Cu alloy [14], (b) Failed Fixed Drive Link component

The percentage of second-phase constituents in Aluminum alloy should be decreased during homogenization. Homogenization can also increase hardness, yield strength, and tensile strength without much change in elongation [15]. Fan Xi-Gang and Jiang Da-Min [15] have observed the fraction of phases other than α dendrite in Al-Zn-Mg-Cu alloys. The fraction of second-phase particle in Al-6,2%Zn-1,7%Cu-2,3%Mg decreases with the function of time and temperature. Fig.21 shows the fraction after various homogenizing time and temperature.

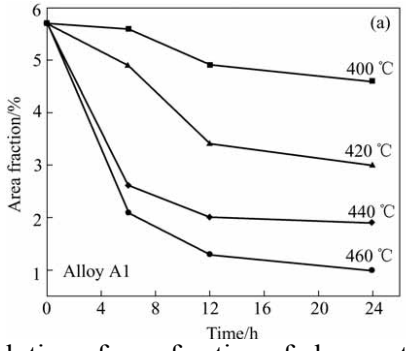

Fig.22 Evolution of area fraction of phases other than α dendrites during heat treatments [15]

Based on data of percentage of insoluble phases shown in Fig.15 and Fig.16, the fraction of insoluble phases in the failed component under stereo quantitative metallography and SEM quantitative metallography, there are 3.06% (area #1) and 3.17% (area #2). This value is higher than the industrial homogenized Aluminum [15]. Fig.15 confirms that the component was not homogenized properly. It could be the homogenizing time was too low or holding time was too short. Whereas, the area far from crack initiation contains insoluble phase lower tnahn that of the area close to crack initiation, as shown in Fig.16, there is 0.76 % (area #a), 0.58 % (area #b), and 0.39 % (area #c), respectively.

The excess of insoluble constituents decreases the mechanical properties and confirmed by the tensile test result on Table 2 and hardness test on Table 3. The constituent particles are brittle and can lead to preferential path for crack advance and reduce fracture toughness [4]. Constituent particles have no strengthening

effect due to non-coherent interface with the matrix and too coarse to interference dislocation movement. The common constituents found in 7X75 alloys are Al_7Cu_2Fe, Mg_2Si, SiO_2, and Al_2CuMg [15].

EDS result in Fig.17 indicates that the constituents are Al_7Cu_2Fe that is common constituents in 7X75 wrought alloys. The SEM and EDS analysis indicates in addition to excess fraction of constituents in the area far from fracture, the structure and constituents are normal. The EDS result in Fig.18 shows the particle with Cu as the main element (63% mass fraction). This particle is uncommon for its composition and size. The size of this particle is more than 50 μm as the maximum size of normal constituents in Aluminum alloy. Since the coarse particle with have size more than 1 μm will deteriorate the fatigue performance [15], this Cu-rich particle has the possibility to reduce the fatigue strength in local surrounding area. This Cu-rich particle did not found in the area far from crack initiation and test result indicated that this particle has no effect on hardness of material.

4. Boeing Recommendation

Service Letter [16] recommends:

1. Detail visually inspect drive links for loose cover plate fasteners and/or cracks in the link body itself every "C" check per MPD 57-610-00 and MPD 4-57-041. If cracks or loose fasteners are found, remove the link and replace it.
2. Ensure the flap moveable fairings are rigged properly [1]. The moveable fairing should not be pulled too tightly or unevenly against the lower surface of the flaps which may result in a fully compressed bulb seal condition. If the flap fairing is pulled up unevenly, the link can be asymmetrically loaded causing increased loading to one side of the link. The reference AMM [1] for the outboard flaps have been revised to provide updated rigging instructions for the fairing itself along with the primary and secondary doors on the #1 & #8 fairings.

5. Conclusion

1. The failure of drive system of secondary door from canoe number 8 on PK-GSI was started due to the breakage of Fixed Drive Link (P/N 65B15694-10).
2. The crack initiation is from Fixed Drive Link.
3. Failure mode is fatigue failure.
4. The tensile strength and hardness of component are below the standard for 7075-T6 alloy.
5. Quantitative stereo metallograph on fraction of constituent particles indicates that the homogenization of the part was not performed well.
6. Quantitative SEM metallograph indicates that the farther, the area is away from the crack initiation, the less, constituent particles are detected.
7. Probably, installation process might not be performed properly, so that asymmetrical load occured.

6. Recommendation

1. The study of Cu-rich particle shown in Fig.7 should be done including the spread and fraction of its particle and its effect to the change of mechanical properties.
2. The stress analysis using FEM is also required to determine the area that most prone to fail.

Acknowledgement

The authors acknowledge Mrs. Dede S Nurbaeti for her support and laboratory practice in GMF AeroAsia.

References

[1] ____. 2011. B747-400 Aircraft Maintenance Manual (AMM). Seattle WA: Boeing Commercial Airplane Group. ATA 27-51-31

[2] ____. 2011. Component Maintenance Manual (CMM) Trailing Edge Flap Track Fairing Drive Support Installation. Seattle WA: Boeing Commercial Airplane Group. ATA 27-51-93

[3] ____. 2007. B747-400 Illustrated Part Catalog (IPC): Trailing Edge Flap System. Seattle WA: Boeing Commercial Airplane Group. ATA 27-51-00

[4] ____.2002. ASM Handbook Vol.2 Properties and Selection: Nonferrous Alloys and Special-Purpose Materials. Material Park. Ohio. USA. ASM international.

[5] ____. ASM handbook Vol. 11 Failure Analysis and Prevention. Material Park. Ohio. USA. ASM international.

[6] ____.2002. ASM Handbook Vol. 9 Metallographic and Microstructure. Material park. Ohio. USA. ASM international.

[7] ____.2002. ASM Handbook Vol. 12 Fractography. Material Park. Ohio. USA. ASM international.

[8] Totten, G.E. and MacKenzie, D.S. 2003. Handbook of Aluminum Volume 1: Physical Metallurgy and Processes. New York: Marcel Dekker. Page 120-194.

[9] Totten, G.E. and MacKenzie, D.S. 2003. Handbook of Aluminum Volume 2: Alloy Production and Materials Manufacturing. New York: Marcel Dekker. Page 120-194. 352-405

[10] Kaufman, G.J. 2000. Introduction to Aluminum Alloys and Temper. Material Park. Ohio. USA: ASM international. Page 77-84

[11] Hatch, John. E. 2005. Aluminum Properties and Physical Metallurgy. American Society for Metals. page 105-133

[12] Sananta Sri, Glorianta. 2010. Engineering Report B7/27-51-0324/ER. Cengkareng. Engineering Service: GMF-AeroAsia.

[13] Senkov, O.N. Bhat, R.B. and Schloz, D. Microstructure and Properties of Cast Ingots of Al-Zn-Mg-Cu Alloys Modified with Sc and Zr. Ohio. USA.

[14] Porter, D.E. and Easterling, K.E. 1996. Phase Transformation in Metals and Alloys. London. Chapman and Hall. Page 207-220

[15] Xi-Gang, Fan. Da-Ming, Jiang. 2005. Evolution of Eutectic Structures in Al-Zn-Mg-Cu Alloys during Heat Treatment. Non-ferrous Metal Society. China.

[16] ____. 2009. Service Letter 747-SL-27-199. Seattle WA: Boeing Commercial Airplane Group. ATA 27-51-90